Original scientific paper

Determination of Service Life of Sintered Powder Metallurgy Gears in Regard to Tooth Bending Fatigue

Srečko Glodež, Marko Šori, Krešimir Vučković, Stjepan Risović

Abstract

The aim of this study is to check the possibility of replacing the pinion gear made of structural steel with the one made of sintered material. The pinion is part of the gear pair mounted in front of the gearbox of the skidder Ecotrac 55V to increase the speed and lower torque. In larger series, powder metallurgy (PM) gears are used as a cost-effective alternative for wrought metal gears in a number of industries including the one producing forest products. The present paper discusses the computational and experimental approach for determining the service life of sintered PM gears in regard to tooth bending fatigue. The proposed computational model is based on the stress-life approach, where the stress field in a gear tooth root is determined numerically using finite element method. The needed material data have been taken from the authors' previous work. Due to the scattering nature of fatigue, the statistic approach has also been considered by presentation of computational results. The experimental procedure was done on a custom made back-to-back gear testing rig. The comparison between computational and experimental results has shown that the proposed computational approach is an appropriate calculation method for estimating the service life of sintered gears regarding tooth root strength. Namely, it has been shown that, in case of proper heat treatment of tested gears, tooth breakage occurred in the interval with 95% probability of failure, which has been determined using the proposed computational model.

Keywords: skidder, service life, sintered powder metallurgy gears, tooth bending fatigue, stress-life approach, back-to-back test rig

1. Introduction

There has been an increased awareness of the need to develop forestry techniques and technologies, which is often expressed through the need of providing convenient technical, environmental and ergonomic features as well as achieving higher profits. Therefore, the development of machines and procedures is an important prerequisite for improving a forestry company's performance in complex terrain or when it comes to specific ways of management in naturally renewable forests. According to Beuk et al. (2007), there are four mayor criteria in terms of suitability of technical and technological solutions: environmental suitability, efficiency, safety, ergonomic suitability.

As a result, it is necessary to design new vehicles for off road travel in forest thinning operations, which are suitable for all cut-to-length, half-tree length and tree-length methods. The first such vehicle for wood skidding from thinnings was the articulated forest tractor IWAFUJI, originated in Japan. Afterwards, in 1987, some of the Croatian local forest units encouraged the structural improvement of domestic equipment and vehicles, especially for thinning operations. The result was a prototype of a new machine in the group of the so called small techniques for wood transportation, middle category skidder Ecotrac 33V. In 1996, Horvat and Sever conducted a research on two agricultural adapted tractors (Torpedo TD 75A and Steyr 9080a) and two middle-size skidders (LPKT 40 and Ecotrac 33V), all of which were intended for wood relocation from thinnings. According to research results, morphologic features of the domestic skidder Ecotrac 33V are much more suitable for such opera-

tions, especially its form index with lower length, width and height than the other researched vehicles.

From 1995 to 2007, during a comprehensive study of Ecotrac 33V done by the Croatian Forests Ltd, several technical-technological problems (engine power, break system, winch), maintenance problems, economic profitability and overall working condition problems have been considered. Desiring to keep the basic dimensions of the skidder tractor Ecotrac 33V and build a new skidder capable of working in forest thinning operations and occasionally in main felling, the development started of the new ECOTRAC 55V tractor (see Fig. 1) equipped with forest winch 2x35 kN and 4x4 drive. The skidder was powered by an air-cooled tricylinder diesel motor DEUTZ, with a working volume of 3236 cm^3, compression factor 20:1, nominal power 40 kW at 3400 min^{-1} and maximum torque of 207 Nm at 1600 min^{-1}. Power transfer was performed by a mechanical transmission: drive motor – coupling – gearbox – transfer box – front and back differentials with individual blockades – final (planetary) reducers mounted on the tractor wheels.

In order to obtain the mobility features of the skidder (Đuka et al. 2016) throughout the thinning operation (length, width, height), while also adapting those required for main felling, such as motor power, a gear pair has been mounted in front of the gearbox to increase speed while lowering torque. The gear pair was added in front of the gearbox due to the limitations of the main gearbox dimensions; as a result, the gearbox was unable to work with greater torque than specified. Therefore, the final reduction had to be carried out through a robust planetary transmission.

The aim of this study is to check the possibility of replacing the pinion gear made of structural steel with the one made of sintered material, which is less expensive because no additional grinding and thermal processing is required.

Fig. 1 Skidder ECOTRAC 55V

Large series production demands a cost-effective process with low waste of material and low energy consumption. If massively produced parts also have a complex geometry and tight tolerances, Powder Metallurgy (PM) should be considered for the production process. Conventional PM production process (automatic die compaction and sintering) has already proven its advantages (low cost, low waste, high accuracy, high strength, etc.) and shown its shortcomings (dimensional change during sintering, uneven porosity), which can now be kept under control with various methods, including alloying elements and compaction tool design and movement (Danninger at al. 2001, Khoei and Bakhshiani 2004). The main characteristic of sintered PM components is the porosity, which is usually not available directly, but in a form of density, which is the main factor for mechanical properties of a final product (Cipolloni at al. 2014). Density is unfortunately affected by numerous factors, which are not only the obvious theoretical density of the base powder and compaction pressure, but also the amount and type of alloying elements, amount and type of lube, sintering atmosphere, time and temperature, cooling rate after sintering, etc (L'Esperance at al. 1996, Khraisat and Nyborg 2004, Bolzoni at al. 2013).

PM components are widely used in motor vehicle industry as oil pump gears and housings, various small component brackets, synchronizer gears and engine gears. The next step is PM power transmission gears (Flodin at al. 2011).

The idea of PM gears dates back to 1985, when researchers in Soviet Union investigated tooth strength of sintered planetary pinions for automobile differential (Dorofeev and Baidala 1985). However, due to low Young`s module and low surface hardness, which led to significant wear, the use of PM gears was limited to low load applications. Investigations of RCF (rolling cycle fatigue) on sintered steel led to selective surface densification of gear flanks, which improved surface hardness and therefore reduced wear (Lawcock 2006, Koide at al. 2008, Bengtsson at al. 2001, Bengtsson at al. 2001a). However, surface densification of gear flanks occurs after sintering, thus causing an additional procedure, which raises the cost of the final product. This, consequently, reduces the economic advantage over conventional gear production with milling or hobbing. Recent development in powder metallurgy production technology increased the strength of final PM products to an interesting level

for PM gears applications without additional procedures (Dlapka at al. 2012, Straffelini at al. 2014).

Usually, when considering tooth breakage, gear drives are dimensioned according to standard ISO 6336:2006 or in accordance with other procedures, which cannot be used for sintered PM gears. However, some information on sintered gear bending load capacity can be found in AGMA 930-A05:2005 information sheet, which contains a complex geometrical analysis to determine the geometry factor for bending strength. Furthermore, the needed parameters of fatigue strength are not given and should be found in available literature or determined experimentally. This paper uses stress life approach to evaluate the fatigue life of sintered gears in terms of the bending stress field in the tooth root. The computational results are then compared with experimental data, obtained on the back-to-back gear-testing rig.

2. Material and geometry

Powder manufacturers are already producing steel metal powders for sintered gears (Höganäs 2015). Based on experience in compaction and sintering, one of such powders was chosen to produce PM gears. It contains 1.47% Cu, 1.69% Ni, 0.50% Mo, 0.29% C and 0.58% of lube with Fe balance. Apparent density of this powder is 3.15 g/cm^3 and Hall flow rate is 29 s / 50 g. This powder was compacted into gear specimens and sintered at 1120 °C for 30 minutes in a controlled 10/90 hydrogen and nitrogen atmosphere. After sintering, PM gears were machined to reduce tooth width and to produce a key slot in the hole (see Fig. 2). Sintered PM gears were then austenitized at 915 °C, oil quenched and tempered for one hour at 175 °C. Final density of specimen gears was 7.03 g/cm^3.

Table 1 Mechanical properties of tested gear (Šori at al. 2014, Šori at al. 2014a)

Property	Value
Young`s module E, GPa	142
Poisson`s ratio ν (Hirose at al. 2004)	0.27
Ultimate tensile strength R_m, MPa	842
Elongation at break A	0.86
Fatigue strength coefficient σ_f`, MPa	875
Fatigue strength exponent b	–0.153

Mechanical properties of sintered gears (see Table 1) were considered the same as those determined in previous mechanical testing of this sintered steel described in our previous work (Šori at al. 2014, Šori at al. 2014a). Although final density of sintered gears was slightly lower than in previous experiments, everything else remained the same as in the mentioned experiments.

Tested sintered pinion with 9 teeth and 5 mm tooth width was paired with wrought carburized tempered steel gear with 31 teeth and 20 mm tooth width at centre distance of 80 mm. Normal module was 4 mm, pressure angle at normal section was 25° and helix angle was zero. Nominal rotational speed of a tested pinion was 800 rpm.

3. Computational estimation of service life

Computational estimated service life of a sintered gear with chosen geometry and known material parameters is determined in relation to the maximum tensile

Fig. 2 Sintered gear after compaction and sintering (left), after machining (middle) and after heat treatment (right)

stress field in the tooth root, from which the number of stress cycles is calculated according to the modified Basquin`s exponential law (Stephens at al. 2001)

$$\sigma_a = \sigma_f' \cdot \left(2 \cdot N\right)^b \quad (1)$$

which gives the correlation between amplitude stress σ_a and the number of stress cycles until failure N. Fatigue strength coefficient σ_f` = 875 MPa and fatigue strength exponent b = −0.153 are material parameters and have been determined previously using rectangular test specimens, which have been produced in the same way as treated sintered gears (compaction, sintering and additional heat treatment). Detailed experimental procedure is described in Šori at al. 2014a. Due to pulsating load regime in the tooth root, amplitude stress σ_a is equal to the half of the maximum Principal stress:

$$\sigma_a = \frac{1}{2} \cdot \sigma_{max} \quad (2)$$

The maximum stress in tooth root σ_{max} can be calculated according to ISO 6336:2006, but in case of PM gears, the tooth root is not dependant on gear tooth tools and can be optimized to the maximum performance (Liu 2011). Some calculation programs, e.g. KISSSoft 2015, also enable extensive profile corrections, but describing the correct tooth root form with various factors can be more difficult than numerical simulation with the existing 3D model, which is used in compaction die preparation. Therefore, the finite element method (FEM) analysis was used to calculate the tooth stress for a given torque load.

In the FEM approach seen in Fig. 3, the gear in question was modelled with one third geometry as Instance 1 and the pairing gear with only one tooth as Instance 2. The contact between them was set at the outermost single contact point. As only the position of contact point is important to tooth root stress field distribution,

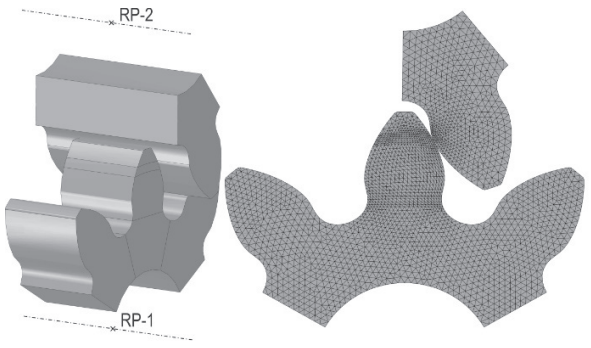

Fig. 3 3D model (left) and mesh (right) of treated gear pair

the pairing tooth of a large gear was substituted with one pinion tooth, but appropriately wider and stiffer. The surfaces of shaft holes and cut result surfaces were tied to each reference point so that all relative displacements and rotations were constrained. At initial step, all degrees of freedom of the reference points were restricted. To apply the load, the reference point of gear pinion instance was rotated in 20 increments for a fraction of a degree to initiate contact between both instances, which caused a reaction moment in the reference point that was considered as load torque for the pinion, which caused stress field in the tooth root. Due to contact, this approach enabled significantly better simulation stability than boundary condition with directly applied torque. Both sections were modelled with linearly elastic material defined with appropriate Young`s modulus $E$ and Poisson`s ratio ν. Contact between the sections was defined as tangentially frictionless and in normal direction as »hard contact«. Both sections were meshed with half a million tetrahedral C3D4H type elements. For more details about numerical approach, see Glodež at al. 2014.

In case of HCF (high cycle fatigue) regime, stress levels are much lower than Yield strength and thus linear material model is sufficiently suitable for such calculation. This assumption makes it possible to find direct linear correlation between load torque T and maximum Principal stress σ_{max}

$$\sigma_{max} = \kappa \cdot T \quad (3)$$

where κ is a correlation coefficient, which is dependent on gear geometry and linear material properties (Young`s module $E$ and Poisson`s ratio ν), and was determined to be 8.4408 m^1mm^2 in our case.

If Eq. 2 is inserted in Eq. 1 and σ_{max} substituted according to Eq. 3, direct correlation between load torque T and estimated number of stress cycles until failure N_{est} can be written as in Eq. 4, which can also be written as an equation of a straight line in Log(T) – Log(N_{est}) plane, as in Eq. 5.

$$\frac{1}{2}\kappa \cdot T = \sigma_f' \cdot \left(2 \cdot N_{est}\right)^b \quad (4)$$

$$T = \frac{2 \cdot \sigma_f'}{\kappa}\left(2 \cdot N_{est}\right)^b \quad (5)$$

Furthermore, when estimating the number of stress cycles until failure, the scatter of dynamic tests should be considered. Usually at least 10 fatigue tests are conducted at the same stress level to determine the scatter and to evaluate stress life with certain probability (Glodež at al. 2013). In such approach, material parameters σ_f` and b can vary in dependence to stress level. Due to low number of data-points in previous mate-

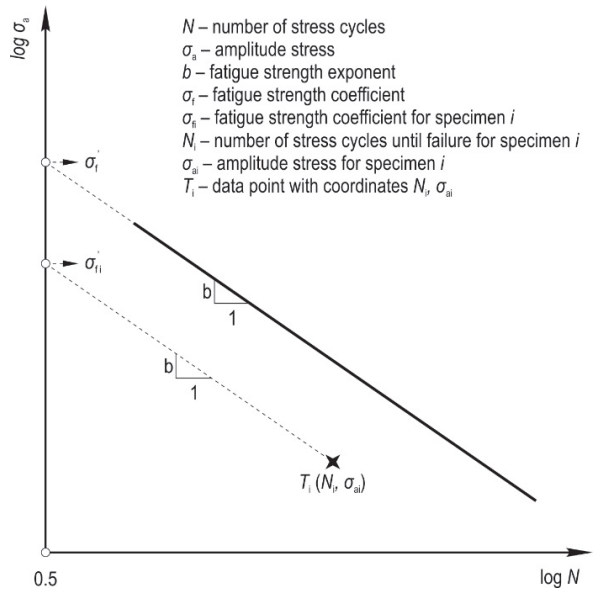

Fig. 4 Definition of $\sigma_{f\,i}^{`}$ for data-point T_i with coordinates (N_i, σ_{ai})

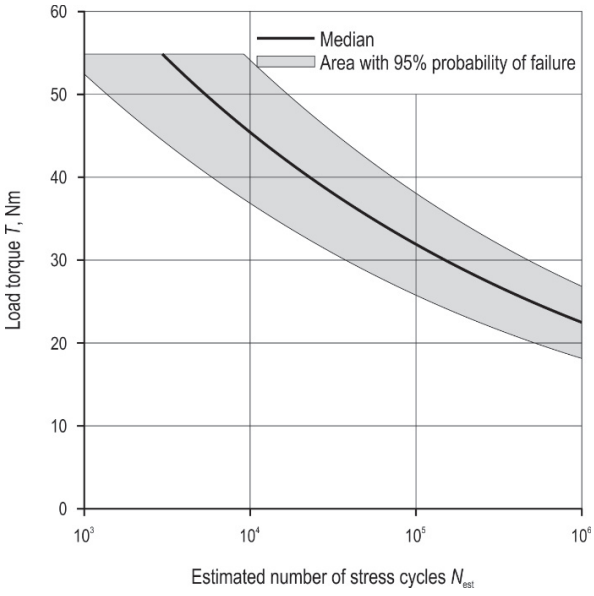

Fig. 5 Area of estimated number of stress cycles N_{est} with 95% probability of failure

rial testing (Šori at al. 2014A), fatigue strength exponent b was assumed to be constant at all stress levels. However, to estimate the area in S-N diagram with 95% probability of failure, fatigue strength coefficient $\sigma_{f\,i}^{`}$ for each data point $T_i$ with coordinates ($N_i$, $\sigma_{ai}$) was calculated in a way schematically shown in Fig. 4. Standard deviation of fatigue strength coefficient $\delta_{\sigma f}$ was then calculated on a set of points $\sigma_{f\,i}^{`}$, making it possible to write Eq. 6, which is Eq. 5 extended with $\pm 2 \cdot \delta_{\sigma f}$.

$$T = \frac{2 \cdot (s_f' + 2 \cdot \delta_{of})}{\kappa} \cdot \left(2 \cdot N_{est}\right)^b \qquad (6)$$

Eq. 6, therefore, defines two curves in $T - N_{est}$ diagram, which are drawn in Fig. 5 also with median curve for our case. Under the lower one, the probability of failure is less than 2.5% and over the upper one, the probability of failure is more than 97.5%. Effectively, they enclose an area with 95% probability of failure.

4. Experimental evaluation of service life

Evaluation of service life was done on a custom made backtoback gear testing rig shown in Fig. 6 with a mechanical torque loop between test gear pair in housing (1) and support gear pair in housing (2). Backtoback configuration enables large testing moments in comparison to the power of a driving motor (3), which only provides rotational movement and covers the

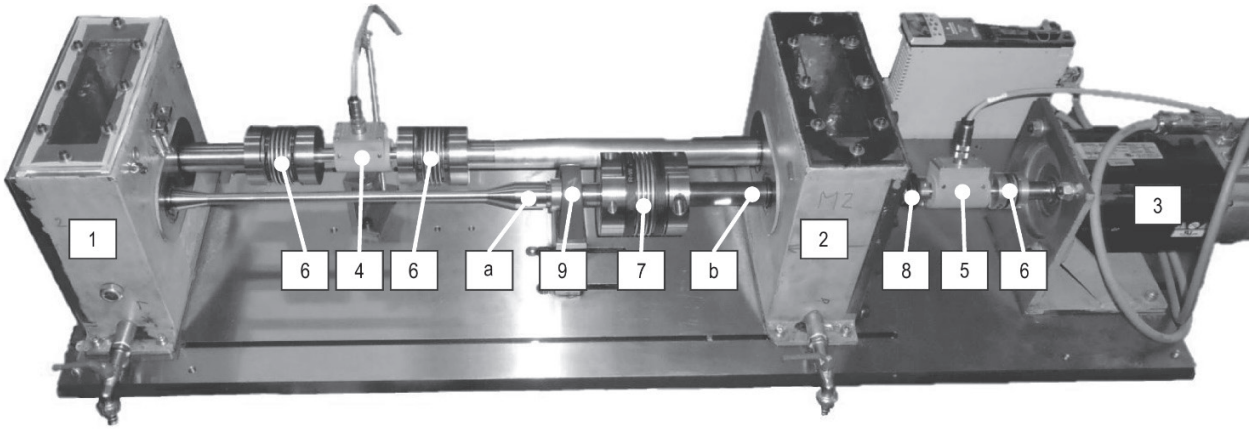

Fig. 6 Custom made gear-testing rig

Table 2 Basic parameters of the testing rig

Parameter	Test pinion	Support gear
Centre distance a, mm	80	
Normal module m, mm	4	
Pressure angle at normal section α_n, °	25	
Helix angle β, °	0	
Width b, mm	5	20
Number of teeth z	9	31
Material	CuNiMo sintered steel	42CrMo4
Nominal rotational speed n, rpm	800	232
Lubrication	Immersed in gearbox oil: ISO VG 220	

losses caused by friction between the gears, in bearings and between gaskets and shafts. Basic parameters of the testing rig are given in Table 2.

Setting the loading torque begins with constraining the shaft rotation near the coupling (7) at position (b). Torque is then applied at position (a), next to support bearing (9). With loading torque applied, coupling (7) is engaged and the mechanical loop is established. The loading torque of the closed loop is monitored with a 200 Nm torque transducer (4), coupled between the shafts with two bellow couplings (6). A smaller 20 Nm torque transducer (5) is used to monitor the exact input torque at the motor (3), which is connected with a bellow coupling (6) to the motor (3) and with a safety bellow coupling (8) to the testing rig. Data acquisition system (DAQ) connects the two torque transducers (4 and 5) to the computer, where measured data are recorded at 50 Hz. This data acquisition rate provides 3.75 measurements per pinion revolution and prevents data overflow at the runout tests – 10^6 pinion revolutions. Data acquisition starts automatically, when the load at smaller 20 Nm torque transducer (5) is more than 2 Nm and also stops automatically, when the torque is lower than 0.5 Nm. If gear breakage occurs, test gears in housing (1) jam and safety coupling (8) disengages.

According to the operation period estimated in the previous section, such loading torque was applied that the expected number of cycles until failure was between 104 and 106. Therefore, the loading torques varied between 22 and 40 Nm – see Table 3. However, the exact setting of the desired torque during the complete test was not possible due to the way of torque application, which does not permit configuration of loading torque during operation of the testing rig. In cases without tooth flank wear, this would not have posed a problem, but with wear of tooth flanks, the loading torque drops. The majority of the tests were done at 800 rpm, which is 33% faster than the fatigue tests on specimens in previous tests. Two tests were also done for higher rotational speed at 1200 rpm for a quick speed dependence evaluation discussed in the following section and are clearly marked in the table.

5. Results and discussion

Results of sintered gear testing are shown in Table 3, where rotational speed, average torque, time and number of cycles are given for each tested sintered gear marked from K01 up to K20. The average torque was calculated from all data points from the beginning of the test until tooth breakage. The time between these two events is also given. The number of cycles was then calculated as a product of rotational speed and time. In the last column, some remarks are given where necessary.

The first four test gears achieved significantly lower operation time as expected and were, therefore,

Table 3 Gear testing results

Specimen	Rotational speed rpm	Average torque Nm	Time min	Number of cycles	Remarks
K01	800	34.3	24.946	19 957	Inappropriate heat treatment
K02	800	28.0	83.179	66 543	
K03	800	28.9	61.223	48 978	
K04	800	27.0	61.898	49 518	
K05	800	22.4	1293.1	1 034 480	Runout
K06	800	34.3	142.55	114 040	
K07	800	39.5	56.885	45 508	
K08	800	31.5	286.94	229 552	
K09	800	28.4	400.80	320 640	
K10	800	26.2	569.79	455 832	
K11	1200	25.0	838.38	1 006 056	Runout
K12	800	29.1	294.36	235 488	
K13	1200	29.6	809.26	971 112	Runout
K14	800	38.3	54.105	43 284	
K15	800	31.6	149.77	119 816	
K16	800	31.3	185.71	148 568	Shaft failure
K17	800	25.8	313.68	250 944	
K18	800	25.2	288.08	230 464	
K19	800	22.2	1258.8	1 007 040	Runout
K20	800	22.6	12504	10 003 200	Runout

subjected to metallographic investigation, where inappropriate heat treatment was discovered, which was caused by an electrical issue in one of the heaters in the furnace for additional heat treatment. Subsequent test gears were then properly heat-treated and tested as seen in Table 3.

All the results, except K20, are plotted in Fig. 7. Regular tests are marked with black dots and are well within 95% probability of estimation, which is the grey area in the diagram. The first four tests with inappropriate heat treatment are marked with black circles and are on the edge of the estimation area. Black cross indicates an irregular test, where shaft failure occurred, but the gear remained intact. All four marks near 106 indicate runouts, but the two triangles are the tests ran at 1200 rpm and one of them is well outside the estimation area. This suggests a speed dependence of fatigue tests. The calculated estimation is based on fatigue tests that were done at 10 Hz, which would result in rotational speed of 600 rpm. The majority of tests were, however, done at 800 rpm, which is 33% more than fatigue tests. On the other side, the tests at 1200 rpm have the double gear meshing frequency of the fatigue tests, which reduces the time of contact and therefore increases the number of stress cycles until failure. This, off course, does not affect the service time, since rotational speed is higher.

Examination of failed test gears showed that all of them had similar damage. Typical damage of a tested gear is shown in Fig. 8, presenting a photo of the test gear K08. Apart from obvious tooth breakage, severe pitting of the working tooth flank can be seen. Although

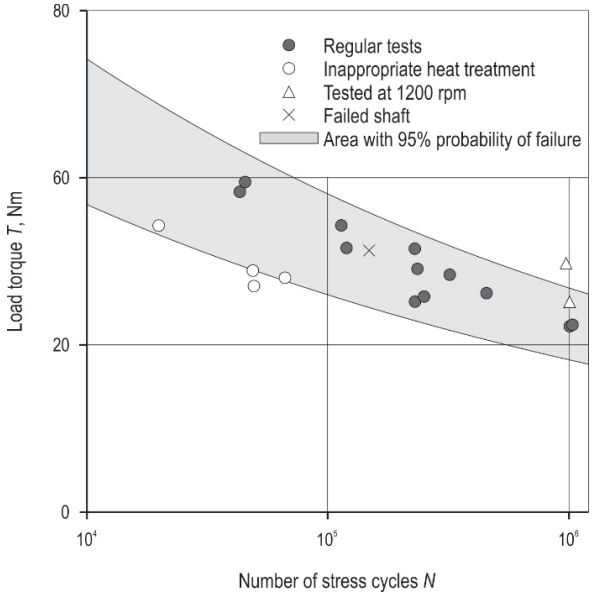

Fig. 7 Gear tests versus calculated estimation of operation period

Fig. 8 Typical damage after test – test gear K08

sintered gears were additionally hardened, the porosity of the material kept hardness relatively low if compared to wrought steel gears, but this can be improved by surface rolling (Sonsino at al. 1992). The hardness of tested gears was measured to be from 310 HV to 340 HV. Significant wear is also visible at tooth tip, which is a result of high sliding velocities and possibly also a consequence of a low Young's module, which could cause meshing interference. Another area of extreme wear is seen at tooth root on a neighbouring tooth. As it is only seen at the neighbouring tooth, this wear can be contributed to unusual meshing conditions right after tooth breakage and before jamming of gears.

6. Conclusions

The aim of research presented in this paper was to compare the computational and experimental approach for determining the service life of sintered PM gears in regard to tooth bending fatigue in order to check the possibility of replacing the steel gear used in skidder ECOTRAC 55V.

The proposed computational model is based on the stress-life approach, where the needed material data was overviewed and referenced to our previous work. The stress field in a gear tooth root was determined numerically using FEM. The experimental determination of service life was done on a custom made back-toback gear testing rig.

The standardized procedure (AGMA 2005) for determining the load capacity of sintered gears requires the calculation of many influential factors that are mainly dependent on gear geometry. FEM analysis may be used to replace this procedure and determine stress field numerically. Usually, dies for sinter-press

technology are made by wire-EDM and at least 2D contour exists, which can be used for quick preparation of a FEM model.

Due to the scattering nature of fatigue, not just a single value is obtained for a particular load, but an interval with arbitrary probability, which is expanded for all torque loads as an area plotted in a load to service time diagram. Due to small number of data points in fatigue tests, standard deviation was calculated based on fatigue strength coefficient σ_f` assuming that fatigue strength exponent *b* remains constant at all load levels.

To validate the proposed approach, the expected service life was calculated with 95% probability of failure with material parameters from our material characterization work (Šori at al. 2014a, Šori at al. 2014b). Sintered pinions were then produced and tested on a custom build back-to-back gear-testing rig until tooth breakage. It was shown that, in case of proper heat treatment, tooth breakage occurred well within the calculated estimation. Therefore, it can be assumed that this approach is an appropriate calculation method for estimating the service time of sintered gears regarding tooth root strength.

The computational model was successfully confirmed with experimental tests on a custom-made gear-testing rig. However, during the evaluation, some further damage, other than gear tooth breakage, was also observed. Presumably, due to relatively low hardness of tooth flanks, severe pitting occurred on the working flanks of sintered gears. Furthermore, some wear was spotted at gear-tooth tips, which may also be a result of low hardness or even improper meshing of gears due to lower Young`s module of the sintered gear. Our future work will, therefore, focus on wear estimation of sintered PM gears. The aim will be to improve the surface hardness with the existing method and to implement sinter-hardening procedure, where sintered parts are hardened right after sintering, thus reducing production time and cost.

Because of great loads on the gearbox of skidder Ecotrac 55V, and considering the obtained results of low tooth root strength and observed tooth flank damage, it can be concluded that the pinion gear made of sintered material is not a suitable replacement for the one made of structural steel.

Acknowledgements

This study was funded by the Slovenian Research Agency in the scope of the Training of Young Researchers programme (grant number: 1000-11-310171) and by Ministry of Science and Education of the Republic of Croatia in the scope of Croatian-Slovenian Scientific and Technological Cooperation.

7. References

AGMA, 930-A05: 2005: Calculated Bending Load Capacity of Powder Metallurgy (P/M) External Spur Gears. American Gear Manufacturers Association. Alexandria, Virginia, U.S.A: 78 p.

Bengtsson, S., Fordén, L., Dizdar, S., Johansson, P., 2001: Surface densified P/M transmission gear. PM01-25: Paper Presented at 2001 International Conference on' Power Transmission Components. Advances in High Performance Powder Metallurgy Applications' Ypsilanti, Michigan, USA, October 16–17.

Bengtsson, S., Fordén, L., Johansson, P., Dizdar, S., 2001a: Rolling contact fatigue tests of selectively densified materials. SAE Technical Paper 2001-01-3285: 10 p.

Beuk, D., Tomašić, Ž., Horvat, D., 2007: Status and development of forest harvesting mechanisation in Croatian state forestry. Croatian Journal of Forest Engineering 28(1): 63–82.

Bolzoni, L., Ruiz-Navas, E. M., Gordo, E., 2013: Influence of sintering parameters on the properties of powder metallurgy Ti-3Al-2.5V alloy. Materials Characterization 84: 48–57.

Cipolloni, G., Menapace, C., Cristofolini, I., Molinari, A., 2014: A quantitative characterisation of porosity in a Cr-Mo sintered steel using image analysis. Materials Characterization 94: 58–68.

Danninger, H., Frauendienst, G., Streb, K.-D., Ratzi, R., 2001: Dissolution of different graphite grades during sintering of PM steels. Materials Chemistry and Physics 67(1): 72–77.

Dlapka, M., Danninger, H., Gierl, C., Klammer, E., Weiss, B., Khatibi, G., Betzwar-Kotas, A., 2012: Fatigue Behaviour and Wear Resistance of Sinter-Hardening Steels. International Journal of Powder Metallurgy 48(5): 49–60.

Dorofeev, Y. G., Baidala, É. S., 1985: Static strength of the teeth of powder metallurgy planetary pinions for the Zhiguli automobile differential. Soviet Powder Metallurgy and Metal Ceramics 24(8): 644–477.

Đuka, A., Pentek. T., Horvat. D., Poršinsky, T., 2016: Modelling of Downhill Timber Skidding: Bigger Load – Bigger Slope. Croatian Journal of Forest Engineering 37(1): 139–150.

Flodin, A., Brecher, C., Gorgels, C., Rothlingshofer, T., Henser, J., 2011: Designing Powder Metal Gears. Gear Solutions 9(101): 26–35.

Glodež, S., Šori, M., Kramberger, J., 2013: Prediction of micro-crack initiation in high strength steels using Weibull distribution. Engineering Fracture Mechanics 108: 263–274.

Glodež, S., Šori, M., Verlak, T., 2014: A Computational Model for Bending Fatigue Analyses of Sintered Gears. Strojniški vestnik – Journal of Mechanical Engineering 60(10): 649–655.

Hirose, N., Asami, J., Fujiki, A., Oouchi, K., 2004: Poisson's Ratio of Sintered Materials for Structural Machine Parts. Journal of the Japan Society of Powder and Powder Metallurgy 51(7): 515–521.

Höganäs, http://www.hoganas.com/. Accessed 6 October 2015.

Horvat, D., Sever, S., 1996: Neke tehničke značajke traktora za privlačenje drva u prorjedama sastojina brdsko-planinskog područja. Šumarski list, znanstveno-stručno i staleško glasilo Hrvatskoga šumarskog društva 120(3–4): 157–162.

ISO, 6336: 2006: Calculation of load capacity of spur and helical gears. International Standard Organization. Geneva, Switzerland.

Khoei, A. R., Bakhshiani, A., 2004: A hypoelasto-plastic finite strain simulation of powder compaction processes with density-dependent endochronic model. International Journal of Solids and Structures 41(22–23): 6081–6110.

Khraisat, W., Nyborg, L., 2004: Effect of carbon and phosphorus addition on sintered density and effect of carbon removal on mechanical properties of high density sintered steel. Materials Science and Technology 20(6): 705–710.

KissSoft A. G., 2015: KissSoft release 03/2015 User manual. Bubikon, Switzerland: 1209 p.

Koide, T., Ishizuka, I., Takemasu, T., Miyachika, K., Oda, S., 2008: Load bearing capacity of surface-rolled sintered metal gears. Int. J. of Automation Technology 2(5): 334–340.

L'Esperance, G., Duchesne, E., De Rege, A., 1996. Effects of materials and process parameters on the microstructure and properties of sinter hardening alloys. Advances in Powder Metallurgy and Particulate Materials 3: 11 p.

Lawcock, R., 2006: Rolling-contact fatigue of surface-densified gears. International Journal of Powder Metallurgy 42(1): 17–29.

Liu, H. R., 2011: The Profile Calculation and the Best Fillet of Powder Metallurgical Gears. Materials Science Forum 694: 851–854.

Sonsino, C. M., Müller, F., Mueller, R., 1992: The improvement of fatigue behaviour of sintered steels by surface rolling. International Journal of Fatigue 14(1): 3–13.

Stephens, R. I., Fatemi, A., Stephens, R. R., Fuchs, H. O., 2001: Metal fatigue in engineering. New York: John Wiley & Sons Inc: 496 p.

Straffelini, G., Benedetti, M., Fontanari, V., 2014: Damage evolution in sinter-hardening powder-metallurgy steels during tensile and fatigue loading. Materials & Design 61: 101–108.

Šori, M., Šuštaršič, B., Glodež, S., 2014: Fatigue properties of sintered DIN SINT-D30 powder metal before and after heat treatment. Materiali in Tehnologije 48(6): 837–840.

Šori, M., Verlak, T., Glodež, S., 2014a: Heat treatment effects on static and dynamic mechanical properties of sintered SINT D30 powder metal. Key Engineering Materials (592–593): 643–646.

Authors' addresses:

Prof. Srečko Glodež, PhD.
e-mail: srecko.glodez@um.si
Marko Šori, PhD.
e-mail: marko.sori@um.si
University of Maribor
Faculty of Mechanical Engineering
Smetanova 17
2000 Maribor
SLOVENIA

Asst. prof. Krešimir Vučković, PhD. *
e-mail: kresimir.vuckovic@fsb.hr
University of Zagreb
Faculty of Mechanical Engineering and Naval Architecture
Ivana Lučića 5
10000 Zagreb
CROATIA

Prof. Stjepan Risović, PhD.
e-mail: risovic@sumfak.hr
University of Zagreb
Faculty of Forestry
Svetošimunska cesta 25
10000 Zagreb
CROATIA

* Corresponding author

Received: December 6, 2017
Accepted: December 18, 2017